Available online at www.sciencedirect.com
SCIENCE DIRECT
International Journal of Mass Spectrometry 253 (2006) 249–255
International Journal of Mass Spectrometry
www.elsevier.com/locate/ijms

Segmental charge distributions of Cytochrome *c* on transfer into the gas phase

K. Breuker *

Institute of Organic Chemistry and Center for Molecular Biosciences Innsbruck (CMBI), University of Innsbruck, Innrain 52a, A-6020 Innsbruck, Austria

Received 21 November 2005; received in revised form 6 April 2006; accepted 11 April 2006
Available online 26 May 2006

Dedicated to Prof. Bernhard Kräutler on the occasion of his 60th birthday.

Abstract

Segmental charge distributions of Cytochrome *c* ions in the transition from solution to gas phase are studied by native electron capture dissociation (NECD). The data suggest that the solution charge distribution of native Cytochrome *c* is partially preserved during the electrospray ionization process. Segments with charge values different from those in solution correspond to protein regions that are the first to unfold on transfer into the gas phase, consistent with an increased gas phase basicity of, and facile proton transfer to, the newly exposed sites. Changes in the charge distribution at elevated temperatures indicate further unfolding, as well as proton transfer as a result of the increased electrostatic interactions in a gas phase environment.

Keywords: Electrospray ionization; Proton transfer

1. Introduction

Protein ions generated by electrospray ionization (ESI) [1] carry multiple charges. For ESI in positive ion mode, the number of charges depends on the structure of the protein in solution, with compact conformations resulting in narrow distributions at lower charge values, and open conformations resulting in broader distributions at higher charge values [2]. Although the protein net charge is evident directly from the *m*/*z* spectrum, the distribution of charges within a protein ion emerging from an ESI droplet is so far unknown. Here the charge distributions within Cytochrome *c* ions in the transition from solution to gas phase are studied by native electron capture dissociation (NECD) [3,4]. Cytochrome *c*, a small electron transfer protein, was also used in a number of studies that discussed the effect of surface accessible area, number of exposed residues, and number of basic versus acidic residues on the net charge of its ESI ions [5]. Equine Cytochrome *c* has 24 basic (R: 2, K: 19, H: 3) and 12 acidic (D: 3, E: 9) residues; the N-terminus is acetylated and the C-terminus carboxylated. Its heme group, covalently bound to the protein chain via thioether linkages at C14 and C17, has two propionate functionalities and an iron center in the Fe^{II} or Fe^{III} state. In aqueous solution at pH 5, equine (Fe^{III})Cytochrome *c* exists in its native structure [6].

In electron capture dissociation (ECD), multiply protonated protein ions stored in the trapped ion cell of a Fourier transform-ion cyclotron resonance (FT-ICR) mass spectrometer react with low-energy electrons to form $\boldsymbol{c}$, $\boldsymbol{z}^{\bullet}$ (∼90%) and $\boldsymbol{a}^{\bullet}$, $\boldsymbol{y}$ product ion pairs [7]. Although $\boldsymbol{a}^{\bullet}$ ions can also be formed by 157 nm photodissociation [8], and $\boldsymbol{y}$ ions (along with $\boldsymbol{b}$ ions) by conventional dissociation methods (e.g., collisionally activated, CAD, or infrared multiphoton dissociation, IRMPD) [9], the $\boldsymbol{c}$, $\boldsymbol{z}^{\bullet}$ ions are unique products of reaction with electrons. The observation of $\boldsymbol{c}$ ions, along with $\boldsymbol{y}$ but no $\boldsymbol{b}$ ions, in ESI spectra of Cytochrome *c* without added electrons was therefore unexpected [3]. The following model of native electron capture dissociation (NECD) was proposed to account for the formation of $\boldsymbol{c}$ and $\boldsymbol{y}$ ions [3]. NECD of (Fe^{III})Cytochrome *c* requires solution concentrations sufficiently high (∼75 μM) for the formation of noncovalently bound homodimers [3]. ESI of such an aqueous dimer solution produces homodimer ions that enter the FT-ICR MS via a heated metal capillary for desolvation, where both

* Tel.: +43 512 507 5240; fax: +43 512 507 2892.
E-mail address: kbreuker@gmx.net.

1387-3806/$ – see front matter © 2006 Elsevier B.V. All rights reserved.
doi:10.1016/j.ijms.2006.04.004

monomers unfold, but one of them (monomer I) faster than the other (monomer II) [4]. This causes proton transfer from the more compact monomer II to the more unfolded monomer I, and induces a substantial charge asymmetry [10]. Whenever the charge asymmetry is sufficiently high (~2:1) [4], two electrons are transferred from monomer II to the heme of monomer I, one reducing the heme iron and the other causing protein backbone cleavage (NECD) next to residues in contact with the heme [3,4]. Thus the NECD fragment ions from a given backbone cleavage site indicate intact noncovalent bonding between the residue next to this cleavage site and the heme, whereas the "missing" cleavages identify regions where the native structure is lost on transfer into the gas phase. For equine (Fe^{III})Cytochrome *c*, the NECD data at different capillary temperatures revealed a sequential unfolding mechanism, with the terminal helices and the 18–34 Ω-loop unfolding first [4]. The order of unfolding of the native (Fe^{III})Cytochrome *c* structure on transfer into the gas phase determined by NECD was found to be essentially the reverse of the order of unfolding in solution [4]. Although the extent of protein hydration at the time when NECD occurs is not known, this implies that the Cytochrome *c* dimers undergoing NECD cannot be fully solvated.

2. Experimental

This study was performed on a 6 T Fourier transform-ion cyclotron resonance (FT-ICR) mass spectrometer described previously [7b]. Ions generated by nano-electrospray in ambient air enter the differentially pumped vacuum system through a heated metal capillary and are transferred into the trapped ion cell by quadrupole ion guides. The capillary temperature was measured at the orifice; no attempt was made to measure the temperature inside the capillary as it cannot be assumed that the protein ions thermalize with the capillary temperature. Electrospray ionization (flow 200–500 nl/min, 1 kV spray potential) utilized emitters (~5 μm inner diameter) made from borosilicate capillaries with a pipette puller (Sutter Instrument Co., Novato, CA). The distance between the emitter and the metal capillary orifice was ~0.5 mm. A platinum wire was inserted into the spray solution from the back of the emitter for application of the spray potential. Equine Cytochrome *c* (Sigma, St. Louis, MO) was dissolved in nanopure water to a final concentration of 75 μM, stirred on a vortex mixer, and stored at 4 °C for 3 months. No buffer was added to the protein solution, as this could affect the charge distributions of the protein ions formed by ESI [11]. All NECD data discussed here were from the same (Fe^{III})Cytochrome *c* solution (all "dimer B", [4]) at pH 5. For each spectrum except that in Fig. 4, a new ESI emitter was loaded with protein solution and the spectrum recorded within 3 min after initiation of the electrospray. The spectrum in Fig. 4 is an average of 32 scans, for which the electrospray lasted 20 min. Mass spectral interpretation utilized the automated THRASH program [12]. Relative ion abundance values were calculated from signal heights divided by the ions charge value, as signal height scales inversely with charge for FT-ICR detection in the low-pressure limit. Average charge values, n_0, were calculated as arithmetic mean values from relative abundance values, $A(n)$, and charge values, n, as $n_0 = \sum nA(n)/\sum A(n)$.

3. Results and discussion

Fig. 1 shows a representative NECD spectrum obtained by nano-electrospray of the aqueous (Fe^{III})Cytochrome *c* solution

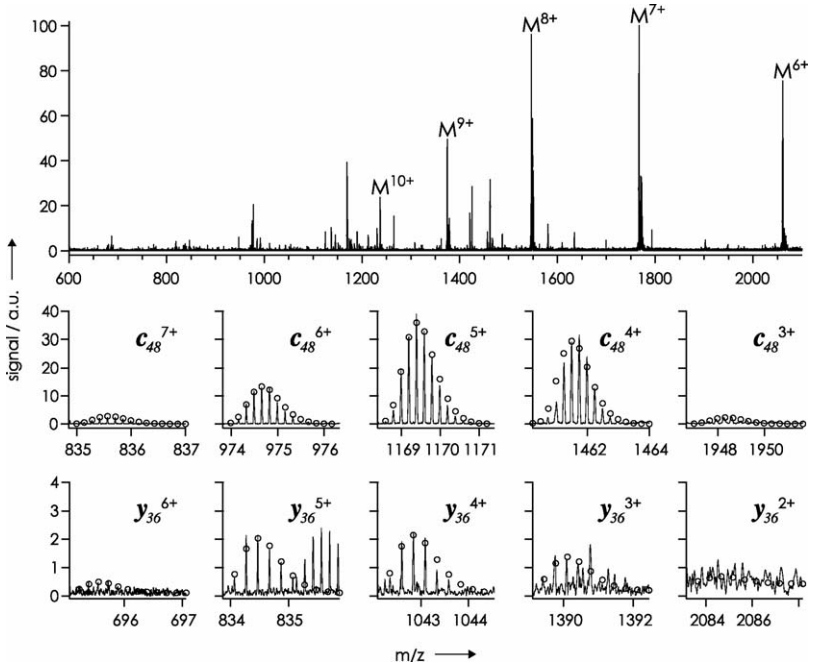

Fig. 1. NECD spectrum of (Fe^{III})Cytochrome *c* from ESI of an aqueous solution (75 μM, pH 5), spray duration 3 min, capillary temperature 38 °C. Bottom traces show enlarged *m/z* ranges for c_{48} for charge values $n = 3$–7 and y_{36} for $n = 2$–6, with calculated isotopic profiles for $[(Fe^{II})c_{48} + nH]^{n+}$ and $(y_{36} + nH)^{n+}$ shown as open circles.

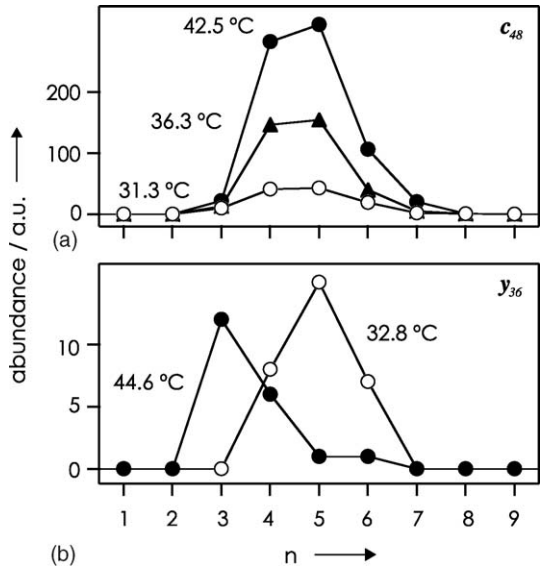

Fig. 2. Relative abundance of NECD fragment ions vs. charge value n; (a) $\boldsymbol{c}_{48}$ at 31.3 °C (open circles), 36.3 °C (triangles), and 42.5 °C (filled circles); (b) $\boldsymbol{y}_{36}$ at 32.8 °C (open circles) and 44.6 °C (filled circles).

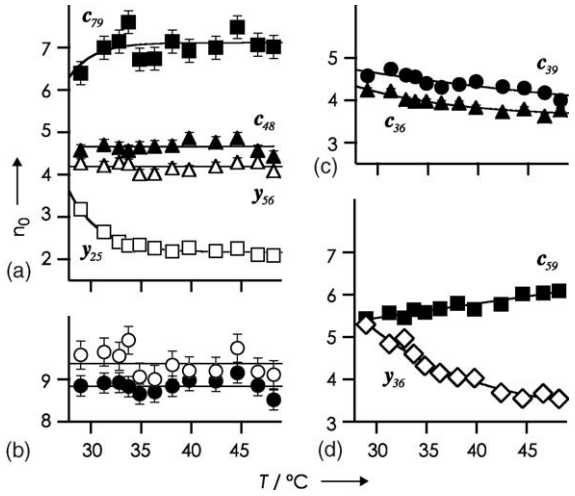

Fig. 3. Average fragment charge values, n_0, vs. capillary temperature for (a) $\boldsymbol{c}_{48}$ (filled triangles), $\boldsymbol{y}_{56}$ (open triangles), $\boldsymbol{c}_{79}$ (filled squares), $\boldsymbol{y}_{25}$ (open squares); (b) added n_0 values of $\boldsymbol{c}_{48}$ and $\boldsymbol{y}_{56}$ (filled circles), $\boldsymbol{c}_{79}$ and $\boldsymbol{y}_{25}$ (open circles); (c) $\boldsymbol{c}_{36}$ (triangles), $\boldsymbol{c}_{39}$ (circles); (d) $\boldsymbol{c}_{59}$ (squares), $\boldsymbol{y}_{36}$ (diamonds); solid lines are to guide the eye.

described in the Section 2. Along with molecular ions, NECD fragment ions from protein backbone cleavage next to amino acids with noncovalent heme contacts in the native structure are observed. Just like the molecular ions, the NECD fragments were detected as ions with a distribution of charge values, illustrated here for $\boldsymbol{c}_{48}$ and $\boldsymbol{y}_{36}$ (lower traces in Fig. 1).

Fig. 2 shows the relative abundance of $\boldsymbol{c}_{48}$ and $\boldsymbol{y}_{36}$ NECD fragment ions versus charge value n for different capillary temperatures. The position of the abundance distributions of $\boldsymbol{c}_{48}$ did not vary significantly with capillary temperature (Fig. 2a), whereas those of $\boldsymbol{y}_{36}$ shifted from higher to lower charge values with increasing temperature. As a consequence, the average charge values, n_0, showed little variation with temperature for $\boldsymbol{c}_{48}$, whereas those of $\boldsymbol{y}_{36}$ decreased with increasing temperature from +5.3 at 29 °C to +3.5 at 48 °C (Fig. 3).

The quasi-complement of $\boldsymbol{c}_{48}$ (residues 1–48) is $\boldsymbol{y}_{56}$ (residues 49–104) [13], whose n_0 values also showed no significant variation with temperature (Fig. 3a). The added n_0 values of $\boldsymbol{c}_{48}$ ($+4.7 \pm 0.2$) and $\boldsymbol{y}_{56}$ ($+4.2 \pm 0.1$) give $+8.9 \pm 0.3$ (Fig. 3b); adding the n_0 values of the quasi-complements $\boldsymbol{c}_{79}$ (residues 1–79) and $\boldsymbol{y}_{25}$ (residues 80–104) gives a less precise, but consistent, value of $+9.4 \pm 0.4$ (Fig. 3b). This indicates an average charge of ~+9 for the precursor of $\boldsymbol{c}_{48}$, y_{56}, $\boldsymbol{c}_{79}$, and $\boldsymbol{y}_{25}$, monomer I. Taking into account the two electrons consumed in backbone cleavage and heme iron reduction [3], the average charge of monomer I before electron transfer was ~+11.

As a general trend, the n_0 values of the smaller fragments ($\boldsymbol{y}_{25}$, $\boldsymbol{y}_{36}$, $\boldsymbol{c}_{36}$, $\boldsymbol{c}_{39}$) decreased, while those of the larger fragments ($\boldsymbol{c}_{59}$, $\boldsymbol{c}_{79}$) increased with increasing temperature (Fig. 3), except for $\boldsymbol{c}_{48}$, $\boldsymbol{y}_{56}$, and $\boldsymbol{c}_{12}$ [14]. This is consistent with the initial unfolding of, and proton transfer to, the terminal helices (residues 1–14, 90–104) and the Ω-loop (residues 18–34), and the competition for protons of other regions at elevated temperatures while retaining the monomer I charge of ~+11 required for electron transfer at all temperatures. The quasi-complementary fragments of $\boldsymbol{c}_{12}$, $\boldsymbol{c}_{36}$, $\boldsymbol{c}_{39}$, $\boldsymbol{c}_{59}$, and $\boldsymbol{y}_{36}$, that is $\boldsymbol{y}_{92}$, $\boldsymbol{y}_{68}$, $\boldsymbol{y}_{65}$, $\boldsymbol{y}_{45}$, and $\boldsymbol{c}_{68}$, respectively (Scheme 1), were either not detected or of too low abundance ($\boldsymbol{y}_{68}$) for the determination of average charge states. Apparently, the branching ratios of $\boldsymbol{c}$ and $\boldsymbol{y}$ products differ widely for different cleavage sites, ranging from $\boldsymbol{c}$ ions only ($\boldsymbol{c}_{12}$, $\boldsymbol{c}_{39}$, $\boldsymbol{c}_{59}$), to 4.4 ± 0.4 ($\boldsymbol{c}_{48}$, $\boldsymbol{y}_{56}$), to 0.7 ± 0.1 ($\boldsymbol{c}_{79}$, $\boldsymbol{y}_{25}$), to y ions only ($\boldsymbol{y}_{36}$), yet without significant variations with temperature (data not shown). These differences could result from conformational or inductive effects that will be addressed in a future study.

Is it possible that the fragment ions for which quasi-complements were not detected or of too low abundance for

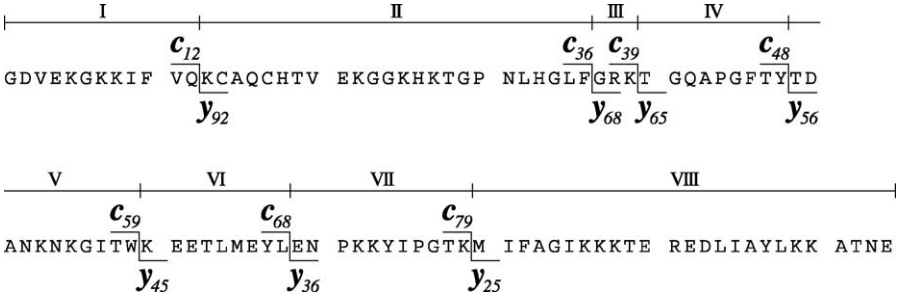

Scheme 1.

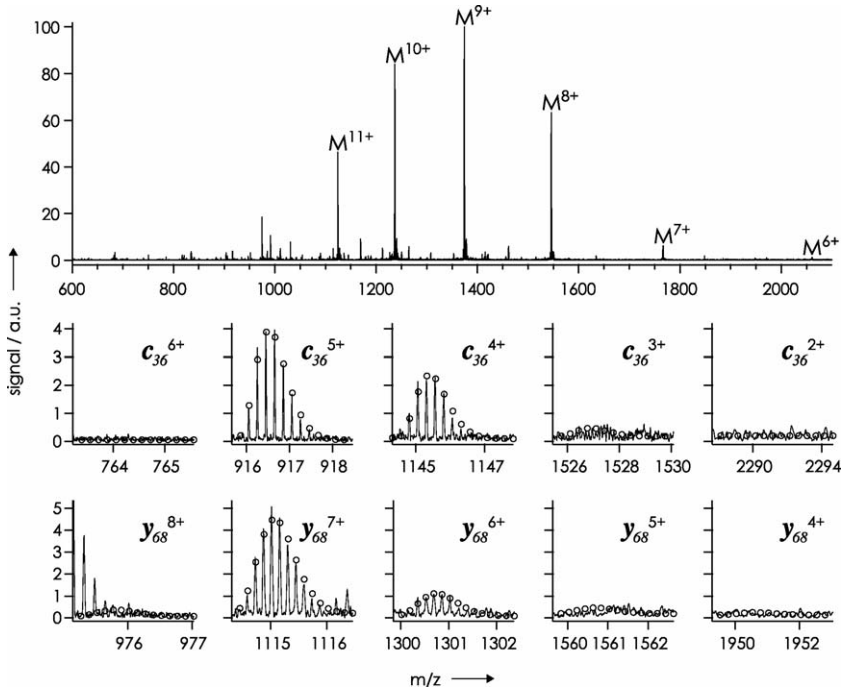

Fig. 4. NECD spectrum of (Fe^{III})Cytochrome *c* from ESI of an aqueous solution (75 μM, pH 5), spray duration 20 min, capillary temperature 36 °C. Bottom traces show enlarged *m/z* ranges for $\boldsymbol{c}_{36}$ for charge values $n = 2$–6 and $\boldsymbol{y}_{68}$ for $n = 4$–8, with calculated isotopic profiles for $[(Fe^{II})\boldsymbol{c}_{36} + n\mathrm{H}]^{n+}$ and $(\boldsymbol{y}_{68} + n\mathrm{H})^{n+}$ shown as open circles.

the determination of average charge states ($\boldsymbol{c}_{12}$, $\boldsymbol{c}_{36}$, $\boldsymbol{c}_{39}$, $\boldsymbol{c}_{59}$, and $\boldsymbol{y}_{36}$) come from monomer I precursors with charge values different from those of $\boldsymbol{c}_{48}/\boldsymbol{y}_{56}$ and $\boldsymbol{c}_{79}/\boldsymbol{y}_{25}$? To test this hypothesis, a spectrum was recorded averaging 32 scans (Fig. 4) for an increased signal-to-noise ratio; here the electrospray lasted for 20 min. The molecular ion charge values in Fig. 4 are higher than in the spectra for Figs. 1–3, indicating a decrease in pH of the ESI solution as a result of oxidation reactions [15]. The fragment ion charge values were also higher than in the spectra for Figs. 1–3, for which the spray duration was limited to 3 min. The average charge values of $\boldsymbol{c}_{36}$, $\boldsymbol{y}_{68}$, $\boldsymbol{c}_{48}$, $\boldsymbol{y}_{56}$, $\boldsymbol{c}_{79}$, and $\boldsymbol{y}_{25}$ in the spectrum for Fig. 4 were 4.4 ± 0.2, 6.5 ± 0.2, 5.3 ± 0.2, 5.2 ± 0.2, 7.8 ± 0.2, and 2.5 ± 0.2, respectively; $\boldsymbol{y}_{92}$, $\boldsymbol{y}_{65}$, $\boldsymbol{y}_{45}$, and $\boldsymbol{c}_{68}$ were not detected. Adding the n_0 values of the quasi-complements $\boldsymbol{c}_{36}/\boldsymbol{y}_{68}$, $\boldsymbol{c}_{48}/\boldsymbol{y}_{56}$, and $\boldsymbol{c}_{79}/\boldsymbol{y}_{25}$, gives 10.9 ± 0.4, 10.5 ± 0.4, and 10.3 ± 0.4, respectively, in good agreement within error limits. Residues F36, Y48, and K79, corresponding to cleavage products $\boldsymbol{c}_{36}/\boldsymbol{y}_{68}$, $\boldsymbol{c}_{48}/\boldsymbol{y}_{56}$, and $\boldsymbol{c}_{79}/\boldsymbol{y}_{25}$, respectively, are far away from each other in the native structure (Fig. 5). The good agreement of the monomer I charge values for these distant cleavage sites indicates a common precursor charge distribution for all NECD cleavage products in a given experiment.

Assuming that fragment separation after backbone cleavage is faster than any further proton transfer reactions, the n_0 values will then reflect the charge distribution within monomer I immediately after electron transfer. This is a reasonable assumption, as electron capture dissociation is faster than intramolecular proton scrambling [7a]. For the protein segments I (residues 1–12), II (residues 13–36), III (residues 37–39), IV (residues 40–48), V (residues 49–59), VI (residues 60–68), VII (residues 69–79), and VIII (residues

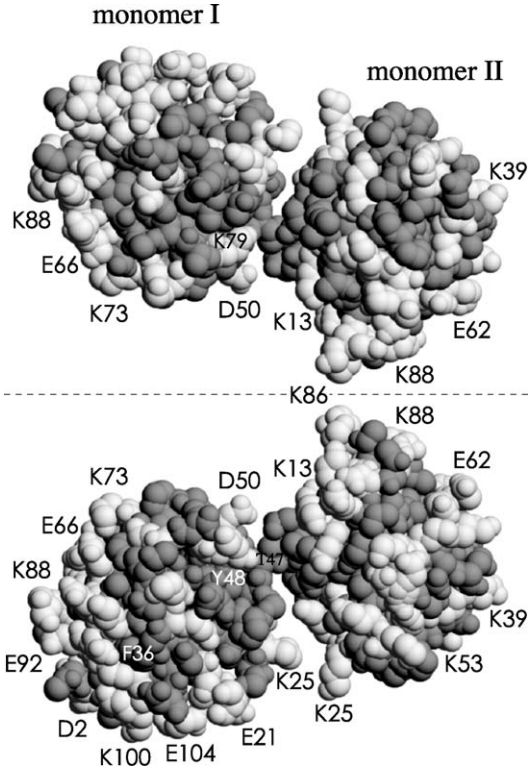

Fig. 5. Asymmetric dimer structure found in crystals of equine (Fe^{III}) Cytochrome *c* at low ionic strength from reference [18]; ionizable residues are shown in light gray. The top and bottom view differ by a 180° rotation around the axis shown as a dashed line.

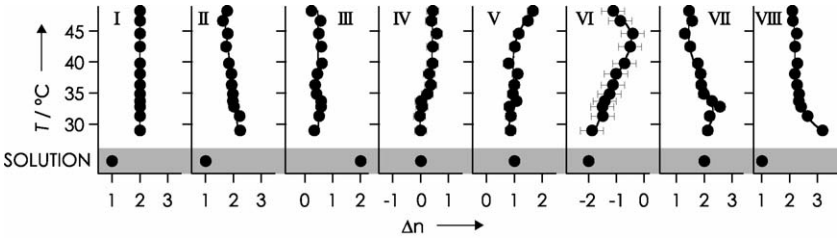

Fig. 6. Average net charge on segments I (residues 1–12), II (residues 13–36), III (residues 37–39), IV (residues 40–48), V (residues 49–59), VI (residues 60–68), VII (residues 69–79), and VIII (residues 80–104), in the temperature range 29–48 °C; solution charge values for the native structure are indicated in the bottom gray region.

80–104) (Scheme 1), average net charges, Δn, were calculated from differences in n_0 values of fragment ions with a shared segment as follows: $\Delta n(\mathrm{I}) = n_0(\boldsymbol{c}_{12})$, $\Delta n(\mathrm{II}) = n_0(c_{36}) - n_0(\boldsymbol{c}_{12})$, $\Delta n(\mathrm{III}) = n_0(\boldsymbol{c}_{39}) - n_0(\boldsymbol{c}_{36})$, $\Delta n(\mathrm{IV}) = n_0(\boldsymbol{c}_{48}) - n_0(\boldsymbol{c}_{39})$, $\Delta n(\mathrm{V}) = n_0(\boldsymbol{c}_{59}) - n_0(\boldsymbol{c}_{48})$, $\Delta n(\mathrm{VI}) = n_0(\boldsymbol{y}_{56}) - n_0(\boldsymbol{y}_{36}) - \Delta n(\mathrm{V})$, $\Delta n(\mathrm{VII}) = n_0(\boldsymbol{y}_{36}) - n_0(\boldsymbol{y}_{25})$, $\Delta n(\mathrm{VIII}) = n_0(\boldsymbol{y}_{25})$; $\boldsymbol{c}_{79}$ was omitted in this analysis because of the larger data scatter (Fig. 3a). The average net charge of segment I was +2 at all temperatures, as only $\boldsymbol{c}_{12}^{2+}$ ions were detected in the NECD spectra. For segment II, Δn decreased slightly from $+2.2 \pm 0.2$ at 29 °C to $+1.8 \pm 0.2$ at 48 °C, whereas no systematic variation with temperature was found for $\Delta n(\mathrm{III}) = +0.5 \pm 0.2$ (Fig. 6). Segment IV showed a small increase in charge from 0.0 ± 0.2 at 29 °C to $+0.4 \pm 0.2$ at 48 °C; the average net charge of segment V was $+1.0 \pm 0.2$ between 29 and 45 °C, and $+1.6 \pm 0.2$ at 47 and 48 °C. The largest change in Δn was found for segments VI and VII, with Δn(VI) increasing from -1.9 ± 0.4 at 29 °C to -0.4 ± 0.4 at 45 °C and then decreasing to -1.1 ± 0.4 at 48 °C, whereas Δn(VII) first increased from $+2.1 \pm 0.2$ at 29 °C to $+2.6 \pm 0.2$ at 33 °C and then decreased to $+1.4 \pm 0.2$ at 48 °C. The average charge on segment VIII decreased from $+3.2 \pm 0.2$ at 29 °C to $+2.1 \pm 0.2$ at 48 °C.

For comparison of the above NECD data with the charge distribution of Cytochrome *c* in the original pH 5 solution, segmental net charges were derived from acid constants of the ionizable groups. The pK_a values for native equine (Fe^{III})Cytochrome *c* from molecular modeling and electrostatic calculations [16] indicate that all aspartic and glutamic acid residues, both heme propionates, and the C-terminus are deprotonated, whereas all lysine and arginine residues are protonated in aqueous solution at pH 5 (Table 1). H18 is not protonated in the native structure as its imidazole *Nε* is coordinated to the heme iron [17]. According to the pK_a values, H26 is also not protonated at pH 5, whereas H33 should be protonated in 50% of the molecules. However, the NMR structure of equine (Fe^{III})Cytochrome *c* shows occupation of the H33 protonation site by a guanidinium hydrogen of R38 [17], so that no positive charge was assigned to H33 here. The heme group contributes two negative charges at the propionate functionalities, and its Fe^{III} center one positive charge. However, the latter charge was ignored in this analysis for ease of comparison with the NECD data; all NECD fragments of (Fe^{III})Cytochrome *c* that include the heme group show reduction to Fe^{II} [3]. The complete charge assignment for equine (Fe^{III})Cytochrome *c* in aqueous pH 5 solution (excluding the heme iron charge) gives net charges of +1, +1, +2, 0, +1, −2, +2, and +1 for segments I, II, III, IV, V, VI, VII, and VIII, respectively (Table 1, Fig. 6). Thus the total charge of native (Fe^{III})Cytochrome *c*, including the charge of the Fe^{III} center, in aqueous pH 5 solution is +7. However, NECD involves noncovalent dimers, not monomers for which the above pK_a values were reported. Based on the NECD fragmentation pattern and order of local unfolding, we have suggested binding of monomer II near Y48/T49 of monomer I in the "dimer B" structure studied here [4]. This binding corresponds to that found in the asymmetric dimer unit in crystals of (Fe^{III})Cytochrome *c* at low ionic strength [18]. In this dimer structure (Fig. 5), all ionizable groups of either monomer are fully solvated and none of them is in contact with the other monomer. Thus it is reasonable to assume that the solution charge distribution for monomers I and II as part of the dimer B structure is the same as for free (Fe^{III})Cytochrome *c* monomers.

For segments IV–VII, the net charges in solution agree, within error limits, with the Δn values at the lowest capillary temperature with which NECD was observed here, 29 °C (Fig. 6). Thus the solution charge of these segments, and especially the −2 charge of segment VI, is initially preserved during transfer into the gas phase. In contrast, segments I and II each carry one more, and segment VIII even two more charges than in solution. Segment III has, at all temperatures, ∼1.5 charges less than in solution, indicating that the proton flow to segments I, II, and VIII is in part supplied intramolecularly. The increased charge on segments I, II, and VIII at 29 °C, together with the preservation of the solution charge on segments IV–VII, is consistent with the terminal helices separating and the 18–34 Ω-loop unfolding as the first step in the sequential unfolding of the newly desolvated native structure [4]. The largest increase in charge with increasing temperature was found for segment VI, which includes glutamates E61, E62, and E66, and carries the highest negative charge density in solution (Table 1). The largest decrease in charge with increasing temperature was found for the neighboring segments VII and VIII, suggesting intramolecular proton transfer from segments VII and VIII to VI caused by the increased electrostatic interactions in a gaseous environment. At 47 and 48 °C, the charge on segment VI decreased again, which could be due to competition for protons caused by unfolding in the neighboring segment V.

The observation with NECD of the desolvation-induced unfolding of Cytochrome *c* monomer as part of a dimer structure is possible because monomer I unfolds faster than monomer II, which causes intermolecular proton and subsequent elec-

Table 1
Calculated pK_a values of ionizable residues in native (Fe^{III})Cytochrome *c* (from reference [16]) and charge assignments at pH 5

Residue	Remark	pK_a	Charge at pH 5	Segment, net charge
N-terminus	Acetylated		0	
G1				
D2		2.6	−1	
V3				
E4		3.8	−1	I (1–12), +1
K5		13.1	+1	
G6				
K7		10.2	+1	
K8		10.9	+1	
I9, F10, V11, Q12				
K13		11.7	+1	
p7 (C14)	Heme propionate opposite C14	2.1	−1	
A15, Q16				
p6 (C17)	Heme propionate opposite C17	0.7	−1	
H18, T19, V20	H18 coordinates heme iron			
E21		3.9	−1	
K22		10.8	+1	II (13–36), +1
G23, G24				
K25		10.0	+1	
H26		4.6	0	
K27		9.8	+1	
T28, G29, P30, N31, L32				
H33	Shares proton with R38	5.0	0	
G34, L35, F36				
G37				
R38	Shares proton with H33	12.9	+1	III (37–39), +2
K39		9.5	+1	
T40, G41, Q42, A43, P44, G45, F46, T47, Y48				IV (40–48), 0
T49				
D50		4.0	−1	
A51, N52				
K53		10.3	+1	V (49–59),+1
N54				
K55		10.4	+1	
G56, I57, T58, W59				
K60		10.9	+1	
E61		3.4	−1	
E62		3.2	−1	VI (60–68), −2
T63, L64, M65				
E66		2.9	−1	
Y67, L68				
E69		0.1	−1	
N70, P71				
K72		9.5	+1	VII (69–79), +2
K73		13.4	+1	
Y74, I75, P76, G77, T78				
K79		11.2	+1	
M80, I81, F82, A83, G84, I85				
K86		10.4	+1	
K87		10.6	+1	
K88		10.4	+1	
T89				
E90		2.6	−1	
R91		14.7	+1	
E92		4.5	−1	VIII (80–104), +1
D93		4.1	−1	
L94, I95, A96, Y97, L98				
K99		10.5	+1	
K100		12.1	+1	
A101, T101, N103				
E104		4.0	−1	
C-terminus		1.3	−1	

tron transfer. For free Cytochrome *c* monomer, there is no other monomer that could provide electrons for NECD cleavage. However, intramolecular proton transfer to the newly unfolded regions of the free monomer, as well as to regions with high negative charge density, can proceed without a change in ion net charge. Thus the conservation of protein ion net charge, which may even agree with the net charge in solution, should not be mistaken for the conservation of native structure and charge distributions in the gas phase ions. Eventually, the structurally rearranged protein ions adopt new stable gas phase conformations, which are currently being investigated by H/D exchange [19], ECD [20], and ion mobility techniques [21].

In conclusion, the charge analysis of NECD fragment ions suggests that the native charge distribution of (Fe^{III})Cytochrome *c* is partially preserved in the electrospray process. However, structural rearrangements as well as increased electrostatic interactions upon protein desolvation cause facile proton transfer to the newly exposed sites in unfolded regions, and to negatively charged residues. Neither the charge distribution of native Cytochrome *c*, nor its native conformation, is stable in a gaseous environment.

Acknowledgments

The author acknowledges generous funding from the Austrian FWF and TWF (grants T229, UNI-0404/158), and discussions with Fred W. McLafferty, Xuemei Han, Mi Jin, Peppe Infusini, Robert Konrat, Bernhard Kräutler, Marc-Olivier Ebert, Thomas Müller, and Michal Steinberg. Instrumentation supported by NIH grant GM16609 to F.W. McLafferty.

References

[1] J.B. Fenn, M. Mann, C.K. Meng, S.F. Wong, C.M. Whitehouse, Science 246 (1989) 64.
[2] (a) S.K. Chowdhury, V. Katta, B.T. Chait, J. Am. Chem. Soc. 112 (1990) 9012;
(b) U.A. Mirza, S.L. Cohen, B.T. Chait, Anal. Chem. 65 (1993) 1;
(c) U.A. Mirza, B.T. Chait, Int. J. Mass Spectrom. 162 (1997) 173;
(d) L. Konermann, D.J. Douglas, Biochemistry 36 (1997) 12296;
(e) L. Konermann, D.J. Douglas, J. Am. Soc. Mass Spectrom. 9 (1998) 1248.
[3] K. Breuker, F.W. McLafferty, Angew. Chem. Int. Ed. 42 (2003) 4900.
[4] K. Breuker, F.W. McLafferty, Angew. Chem. Int. Ed. 44 (2005) 4911.
[5] (a) N. Felitsyn, M. Peschke, P. Kebarle, Int. J. Mass Spectrom. 219 (2002) 39;
(b) R. Grandori, J. Mass Spectrom. 38 (2003) 11;
(c) V.J. Nesatyy, M.J.F. Sutter, J. Mass Spectrom. 39 (2004) 93;
(d) I.A. Kaltashov, A. Mohimen, Anal. Chem. 77 (2005) 5370;
(e) H. Prakash, S. Mazumdar, J. Am. Soc. Mass Spectrom. 16 (2005) 1409.
[6] (a) Y. Goto, Y. Hagihara, D. Hamada, M. Hoshino, I. Nishii, Biochemistry 32 (1993) 11878;
(b) Y.O. Kamatari, T. Konno, M. Kataoka, K. Akasaka, J. Mol. Biol. 259 (1996) 512.
[7] (a) R.A. Zubarev, N.L. Kelleher, F.W. McLafferty, J. Am. Chem. Soc. 120 (1998) 3265;
(b) R.A. Zubarev, D.M. Horn, E.K. Fridriksson, N.L. Kelleher, N.A. Kruger, M.A. Lewis, B.K. Carpenter, F.W. McLafferty, Anal. Chem. 72 (2000) 563;
(c) F.W. McLafferty, D.M. Horn, K. Breuker, Y. Ge, M.A. Lewis, B. Cerda, R.A. Zubarev, B.K. Carpenter, J. Am. Soc. Mass Spectrom. 12 (2001) 245.
[8] M.S. Thompson, W. Cui, J.P. Reilly, Angew. Chem. Int. Ed. 43 (2004) 4791.
[9] (a) S.A. McLuckey, D.E. Goeringer, J. Mass Spectrom. 32 (1997) 461;
(b) J. Laskin, J.H. Futrell, Mass Spectrom. Rev. 22 (2003) 158;
(c) R.C. Dunbar, Mass Spectrom. Rev. 23 (2004) 127.
[10] J.C. Jurchen, E.R. Williams, J. Am. Chem. Soc. 125 (2003) 2817.
[11] U.H. Verkerk, M. Peschke, P. Kebarle, J. Mass Spectrom. 38 (2003) 618.
[12] D.M. Horn, R.A. Zubarev, F.W. McLafferty, J. Am. Soc. Mass Spectrom. 11 (2000) 320.
[13] The real complement of $\boldsymbol{c}_{48}$ is $\boldsymbol{z}_{56}^{\bullet}$, but the highly reactive and thermally labile radical $\boldsymbol{z}^{\bullet}$ ions were not detected in the NECD spectra; the same is true for the radical $\boldsymbol{a}^{\bullet}$ ions. However, it is reasonable to assume that the charge states of $\boldsymbol{z}_i^{\bullet}$ and $\boldsymbol{y}_i$ ions are the same.
[14] $\boldsymbol{c}_{12}$ was detected as $\boldsymbol{c}_{12}^{2+}$ only.
[15] G.J. Van Berkel, K.G. Asano, P.D. Schnier, J. Am. Soc. Mass Spectrom. 12 (2001) 853.
[16] M.A. Miteva, G.P. Kossekova, B.O. Villoutreix, B.P. Atanasov, J. Photochem. Photobiol. B: Biol. 37 (1997) 74.
[17] L. Banci, I. Bertini, H.B. Gray, C. Luchinat, T. Reddig, A. Rosato, P. Turano, Biochemistry 36 (1997) 9867.
[18] R. Sanishvili, K.W. Volz, E.M. Westbrook, E. Margoliash, Structure 3 (1995) 707.
[19] (a) D. Suckau, Y. Shi, S.C. Beu, M.W. Senko, J.P. Quinn, F.M. Wampler, F.W. McLafferty, Proc. Natl. Acad. Sci. U.S.A. 90 (1993) 790;
(b) T.D. Wood, R.A. Chorush, F.M. Wampler, D.P. Little, P.B. O'Connor, F.W. McLafferty, Proc. Natl. Acad. Sci. U.S.A. 92 (1995) 2451;
(c) S.J. Valentine, A.E. Counterman, D.E. Clemmer, J. Am. Soc. Mass Spectrom. 8 (1997) 954;
(d) S.J. Valentine, D.E. Clemmer, J. Am. Chem. Soc. 119 (1997) 3558;
(e) F.W. McLafferty, Z.Q. Guan, U. Haupts, T.D. Wood, N.L. Kelleher, J. Am. Chem. Soc. 120 (1998) 4732.
[20] (a) D.M. Horn, K. Breuker, A.J. Frank, F.W. McLafferty, J. Am. Chem. Soc. 123 (2001) 9792;
(b) K. Breuker, H.-B. Oh, D.M. Horn, B.A. Cerda, F.W. McLafferty, J. Am. Chem. Soc. 124 (2002) 6407;
(c) H.-B. Oh, K. Breuker, S.K. Sze, Y. Ge, B.K. Carpenter, F.W. McLafferty, Proc. Natl. Acad. Sci. U.S.A. 99 (2002) 15863;
(d) K. Breuker, H.-B. Oh, C. Lin, B.K. Carpenter, F.W. McLafferty, Proc. Natl. Acad. Sci. U.S.A. 101 (2004) 14011.
[21] (a) D.E. Clemmer, R.R. Hudgins, M.F. Jarrold, J. Am. Chem. Soc. 117 (1995) 10141;
(b) K.B. Shelimov, D.E. Clemmer, R.R. Hudgins, M.F. Jarrold, J. Am. Chem. Soc. 119 (1997) 2240;
(c) C.S. Hoaglund-Hyzer, A.E. Counterman, D.E. Clemmer, Chem. Rev. 99 (1999) 3037;
(d) S. Myung, E.R. Badman, Y.J. Lee, D.E. Clemmer, J. Phys. Chem. A 106 (2002) 9976;
(e) E.W. Robinson, E.R. Williams, J. Am. Soc. Mass Spectrom. 16 (2005) 1427;
(f) E.R. Badman, S. Myung, D.E. Clemmer, J. Am. Soc. Mass Spectrom. 16 (2005) 1493.